Origin of 3.45 eV Emission Line and Yellow Luminescence Band in GaN Nanowires: Surface Microwire and Defect

Pu Huang,[†] Hua Zong,[†] Jun-jie Shi,[*,†] Min Zhang,[‡] Xin-he Jiang,[†] Hong-xia Zhong,[†] Yi-min Ding,[†] Ying-ping He,[†] Jing Lu,[†] and Xiao-dong Hu[†]

[†]State Key Laboratory for Mesoscopic Physics and Department of Physics, Peking University, Beijing 100871, People's Republic of China and [‡]College of Physics and Electronic Information, Inner Mongolia Normal University, Hohhot 010022, People's Republic of China

ABSTRACT The physical origin of the strong emission line at 3.45 eV and broadening yellow luminescence (YL) band centered at 2.2 eV in GaN nanowire (NW) has been debated for many years. Here, we solve these two notable issues by using state-of-the-art first-principles calculations based on many-body perturbation theory combined with polarization-resolved experiments. We demonstrate that the ubiquitous surface "microwires" with amazing characteristics, *i.e.*, the outgrowth nanocrystal along the NW side wall, are vital and offer a new perspective to provide insight into some puzzles in epitaxy materials. Furthermore, inversion of the top valence bands, in the decreasing order of crystal-field split-off hole (CH) and heavy/light hole, results in the optical transition polarized along the NW axis due to quantum confinement. The optical emission from bound excitons localized around the surface microwire to CH band is responsible for the 3.45 eV line with $E \| c$ polarization. Both gallium vacancy and carbon-related defects tend to assemble at the NW surface layer, determining the broadening YL band.

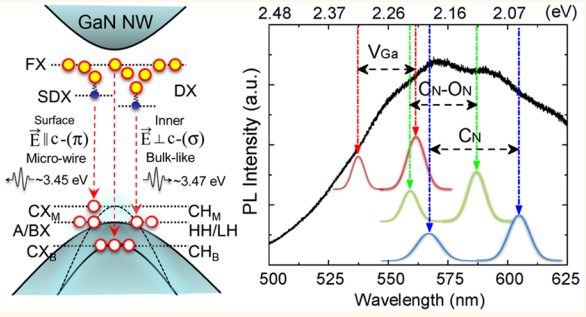

KEYWORDS: GaN nanowire · surface microwire · exciton · defect · first-principles calculations

Technological advancements in GaN nanowires (NWs) have made them promising candidates for applications in light-emitting diodes (LEDs), laser diodes (LDs), transistors, and solar cells.[1−4] In comparison with GaN bulk, the NWs are believed to overcome many limitations such as lattice mismatch with substrate, adsorbate, and dislocation.[5,6] In fact, NW geometry inhibits the propagation of dislocations along its axis, and the free surface permits an efficient elastic relaxation of atoms.[7] Hence, NW structure has been the subject of extensive interest during the past decades. Although the electronic structure and optical properties of GaN NWs have been investigated in recent years, some unresolved challenges still exist. The most notable controversies are the origins of the optical transition at 3.45 eV and the defect-induced yellow luminescence (YL) band centered at 2.2 eV in GaN NWs,[8,9] which have been debated for many years but remain unclear at present.

Generally, the emission line at 3.45 eV is easily observed in GaN NWs with diameters less than 100 nm.[10] It was first observed and recognized as the interstitial Ga inside the NWs.[8] On the basis of time-resolved photoluminescence (PL) experiments, Corfdir *et al.*[11] ascribed this emission to two-electron satellite (TES) caused by the donors located near the NW surface and refuted the attribution of excitons bound to inversion domain boundary suggested by Robins and co-workers.[12] Considering that GaN NWs are usually grown under the N-rich condition and reduction of 3.45 eV emission intensity can be observed if increasing III/V ratio or doping with Mg, Furtmayr *et al.*[13] attributed this line to the surface Ga vacancy (V_{Ga}). Lefebvre *et al.*[14] found that the strength of this emission becomes larger for low-density and small diameter GaN NWs. They thus believe that the NW surface effect is the origin of the 3.45 eV line. Brandt *et al.* also suggested that this emission line originates from surface point defects.[15] Most

* Address correspondence to jjshi@pku.edu.cn.

Received for review July 7, 2015 and accepted August 22, 2015.

Published online August 24, 2015
10.1021/acsnano.5b04158

© 2015 American Chemical Society

recently, Sam-Giao *et al.* fabricated GaN NWs with plasma-assisted molecular beam epitaxy (PA-MBE) and conducted a detailed study of the 3.45 eV emission line by polarization-resolved luminescence and magneto-luminescence experiments. Their results directly refuted Corfdir's claim of TES.[10] The above statements clearly indicate that the origin of this emission line has become a fierce controversy during the past 15 years but is still poorly understood. Hence, an in-depth research is needed to clarify this key issue.

Recently, Li and Wang[16] observed a high-brightness YL band at 566 nm in triangle GaN NWs. Xu *et al.*[9] also found a strong broadening YL emission in hexagonal polar GaN NWs, whereas it disappears in triangular nonpolar GaN NWs. Generally, the YL in GaN is considered as a deep-level transition. Unfortunately, the YL induced by deep acceptors remains controversial. Li and Waag suggested that the $V_{Ga}-O_N$ defect complex could enhance the YL emission as a deep acceptor.[17] The carbon-related defect C_N or its defect complex were also regarded as the origin of the YL.[18,19] Moreover, the V_{Ga}, $V_{Ga}-C_{Ga}$, and Si_{Ga} were supposed as the main contributors to YL.[16,20−22] Most recently, Demchenko *et al.* ascribed the YL to C_N-O_N defect complex in GaN based on density functional theory (DFT) calculations.[23] Xu *et al.* suggested the carbon-related defects may play a key role in the YL emission in GaN NWs.[9] Hence, a persuasive theoretical explanation for the broadening YL band in GaN NWs is still lacking.

In this paper, we find that optical transition from bound excitons localized around the surface outgrowth "microwire" to crystal-field split-off hole (CH) band is the essence of the observed 3.45 eV emission line with **E**∥*c* polarization. The light emissions between exciton and charged defects (gallium vacancy and carbon-related defects) assembled at the NW surface layer determine the broadening YL band. We thus clarify the physical origin of the 3.45 eV emission line (YL band) related to surface microwires (defects).

RESULTS AND DISCUSSION

The surface morphology of self-assembled GaN NWs with diameters from hundreds of nanometers to several micrometers is usually irregular. Ideally, the morphology of GaN NWs orientated along the [0001] direction reveals hexagons with six vertical sidewall facets. Nevertheless, the local growth environment for every NW cannot remain exactly the same, which naturally results in slight differences of growth rate for each facet. Those facets with faster growth rate will force the edge outward, leading to the morphology evolution of GaN NWs from hexagon to triangle or quadrangle. Figure 1a clearly shows that the morphologies of the NWs change from hexagon to triangle or quadrangle, resulting in the formation of the surface outgrowth nanocrystal termed surface microwire in order to distinguish it from the inner bulk-like structure. In comparison with the inner

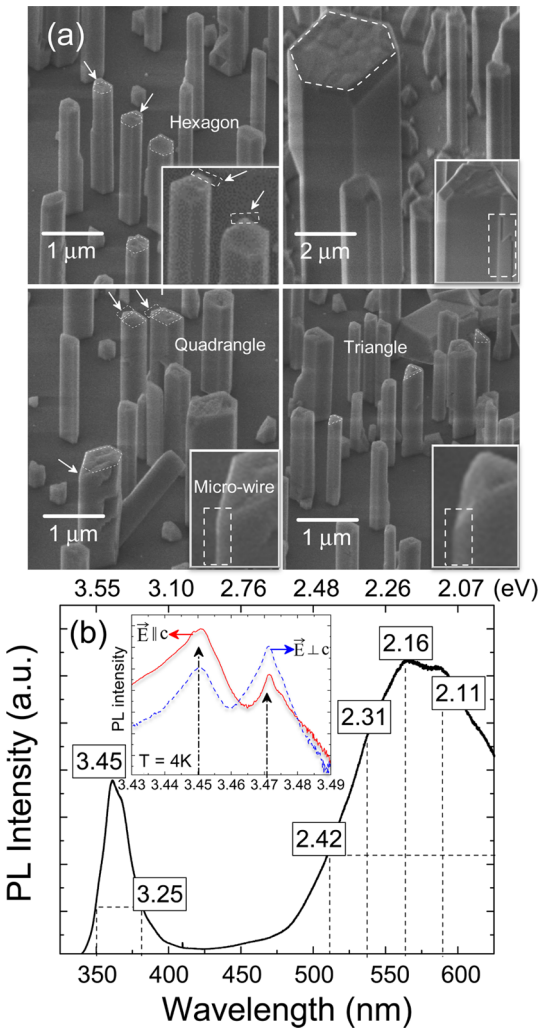

Figure 1. Scanning electron microscopy (SEM) images of GaN NWs grown by the self-assembled process on sapphire substrates (a) and the typical PL spectrum (b). The surface outgrowth nanocrystal along GaN NW side wall, termed surface "microwire", can be observed. The inset of panel b shows the strong polarized light emission with E∥*c* at 3.45 eV in GaN NWs.[10]

GaN NWs, the surface GaN microwire is directly exposed to vacuum, leading to its electronic characteristics completely different from the inner bulk-like GaN. As a matter of fact, the quantum confinement is extremely significant in these surface microwires owing to their nanoscale size.

Figure 1b indicates the typical PL spectrum of these GaN NWs with the strong emission line at 3.45 eV and the broadening YL band centered at 2.2 eV. Generally, the GaN NWs fabricated by metal−organic chemical vapor deposition (MOCVD) with the size from hundreds of nanometers to several micrometers usually have both of these emissions. The disappearance of YL occurs mostly in high-quality GaN NWs, especially for those with diameter within several tens of nanometers. It seems that the YL is dependent on the NW size and becomes weaker with the decreasing NW diameter. Nevertheless, the real physical reason is that the YL,

closely related to the surface gallium vacancy and carbon impurities in GaN NWs (see Figure 6 and its discussion), has a stronger intensity in thick NWs than in thin NWs.[9,16,24] The large surface area in thick NWs provides a region for the defects to gather and permits an efficient elastic relaxation of atoms for stress release. Therefore, defects are inclined to assemble at the NW surface layer, leading to a defect concentration higher than that in the interior. As for those thin GaN NWs, significant lattice distortion will be caused by the defects, resulting in a large formation energy and instability of the whole structure. Hence, these less defect-involved GaN NWs with small diameter are either weak in YL or YL-free.

On the basis of our experimental conditions, we know that the gallium vacancy defects and carbon impurities should be major contributors for the PL of GaN NWs (see the following analyses for details). Meanwhile, one-dimensional (1D) quantum confinement will also play a key role in the optical transitions. Hence, our following discussion is focused on the influence of 1D quantum confinement and defects on the electronic structures and optical properties of GaN NWs, revealing the light emission mechanism at the microlevel.

Figure 2 shows our band gaps for the hexagonal GaN NWs with diameters from 1 nm to infinity, calculated using precise DFT-1/2, GW, and Heyd–Scuseria–Ernzerhof (HSE) methods to overcome the band gap underestimation in the conventional DFT.[25−29] We can see from Figure 2 that our calculated band gap of GaN bulk is in excellent agreement with the previous experimental and theoretical values.[30−32] The gaps determined by DFT-1/2, GW, and HSE are 3.52, 3.50, and 3.41 eV, which are larger than the GGA result (1.99 eV). Our GW calculations predict band gap of 4.85 eV in hexagonal GaN NW (1 nm), which is slightly larger than the HSE result (4.66 eV).[33] Compared with GaN bulk, 1D quantum confinement dramatically increases electronic band gap ~1.4 eV for the NW (1 nm). Our calculations further show that the exciton binding energy decreases remarkably with increasing NW diameter.

The calculated imaginary part of the dielectric functions, closely related to the optical absorption, is shown in Figure 3 for the hexagonal GaN NWs. The optical absorption occurs at 3.34 eV within the UV-A region. The exciton binding energy, given by the difference between the electronic and optical band gaps, is found to be 1.51 eV in GaN NW, which is much larger than that in GaN bulk (23 meV).[34] This is because of the strong 1D quantum confinement and incomplete dielectric screening in small diameter GaN NWs.

To understand the characteristics of polarized absorption around 3.45 eV in depth, we performed polarization-resolved luminescence experiments by focusing the laser on the NW side wall (see Figure 4a). We can find from Figure 4 that the light emission around

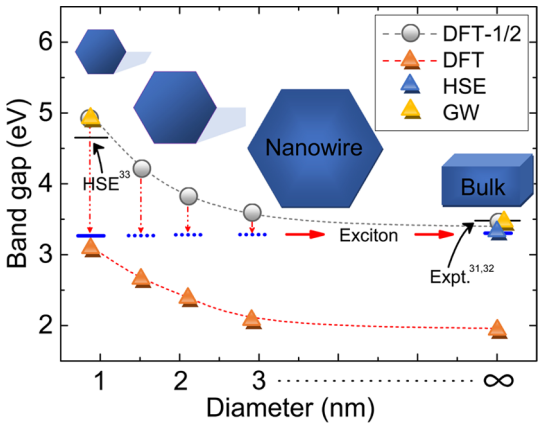

Figure 2. Band gap and exciton energy of hexagonal GaN NWs as a function of the NW diameter.

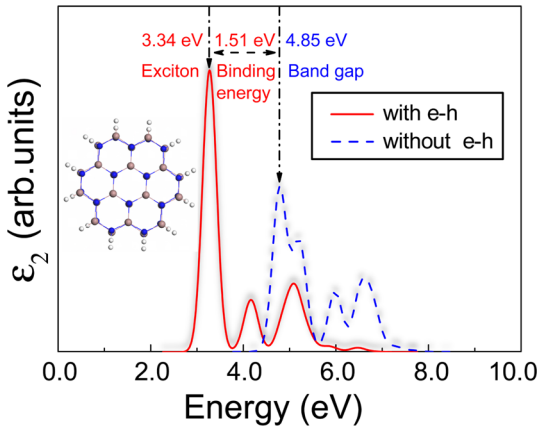

Figure 3. Calculated imaginary part of the dielectric function ε_2 for the hexagonal GaN NW with and without the electron–hole (e–h) interaction.

3.45 eV (360 nm) exhibits a red-shift of 19 nm (0.18 eV) with stronger intensity from $\mathbf{E} \perp c$ to $\mathbf{E} \parallel c$. Our corresponding calculations for the exciton polarized absorption reveal the red-shift of 0.2 eV, which is in good agreement with our PL data.

The detailed calculations for the electronic structures and optical transitions in GaN NWs are shown in Figure 5. The domination of nitrogen p_z state at valence band maximum (VBM) shown in Figure 5a suggests the higher excitation possibility of electrons distributed along the *c*-axis, which directly determines the polarization of light emission and absorption at Γ point in GaN NWs. An inversion of top valence bands in the decreasing order of the crystal-field split-off hole (CH) and heavy/light hole (HH/LH) bands can be induced with decreasing NW diameter. The energy difference between the inverted bands changes from 180 to −27 meV with the NW diameter from 1 nm to infinity (see Figure 5b), which is consistent with previous results for small diameter GaN NWs.[35] It is the band reordering that affects the selection rules of optical transitions and makes the polarization of emitted photons switch from $\mathbf{E} \perp c$ in GaN bulk to $\mathbf{E} \parallel c$ in thin

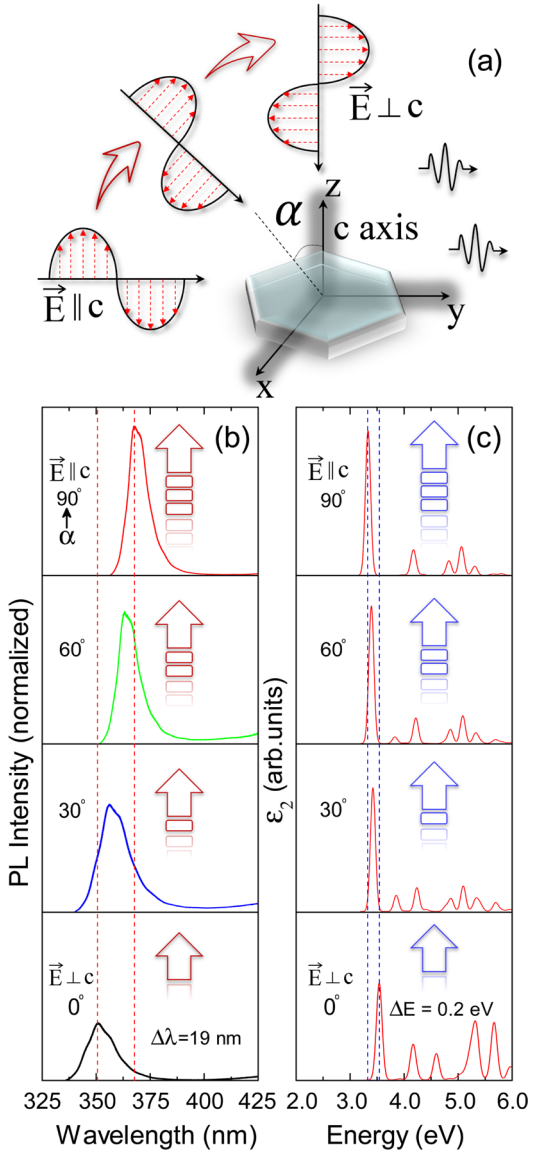

Figure 4. Schematic representation of polarization with different collection angle to NW axis (a), the polarized PL (b), and the calculated polarized exciton absorption (c) in GaN NWs.

GaN NWs (<6.5 nm), resulting in optical emission polarized along the NW axis. The partial density of states (DOS) and distribution of electron wave functions shown in Figure 5a,c provide the most direct evidence for the valence band inversion. We thus know that the 1D quantum confinement significantly modifies the electronic structures and dominates the optical transitions in thin GaN NWs.

GaN NWs fabricated by self-assembled growth with MBE or MOVPE usually have diameters from several tens to hundreds of nanometers,[10,15,24] which indicates the aforementioned valence band inversion can not be observed in these large diameter NWs. Nevertheless, the 3.45 eV transition observed in these NWs has a different dipole orientation with respect to the DX(A) line (3.47 eV) and presents a polarization degree along the *c*-axis.[10] This clearly indicates that some typical surface microstructures should exist in these GaN NWs. On the basis of the observed surface microwire in Figure 1a and the valence band inversion (see Figure 5b), we suggest the 3.45 eV emission should originate from the transition between the bound excitons localized around the surface microwire and CH band. In fact, the surface electron wave functions, which are responsible for the polarization properties of the optical transitions, are essentially altered from *c*-plane to *c*-axis (see Figure 5c) owing to the formation of the surface microwire. This directly leads to the enhancement of parallel polarization (**E**∥*c*) at the NW side wall. Our polarization-resolved experiments and calculations in Figure 4b,c also prove that the emission around 3.45 eV favors coupling to the optical polarized modes with the increasing degree from **E**⊥*c* to **E**∥*c*.

We now discuss the previous notable hypothesis of the surface Ga vacancy for the 3.45 eV emission in GaN NWs under the N-rich condition.[13] It should be noted that this emission is detected only in part of GaN NWs with small diameter. It is impossible that the Ga vacancy exists only in these GaN NWs and none in the others. Moreover, this emission should follow the same polarization selection rules with the DX(A) line if it is caused by the surface Ga vacancy.[10] In other words, the isolated Ga vacancy can not result in the valence band inversion. Hence, we can confirm the 3.45 eV emission originates from the surface microwire along the GaN NW side wall (see Figure 5d) rather than the surface Ga vacancy. This is the essential origin of this emission line and the reason why NW geometry favors coupling to the electromagnetic modes polarized along the NW axis. We thus offer an in-depth explanation for this notable issue.

In fact, the aforementioned surface microwire or microstructure widely exists in epitaxially grown samples, which can significantly alter their electronic structures and characteristics. For instance, previous epitaxial InN films usually exhibit surface irregularity with many surface needle- or wire-like nanocrystals.[36−38] Our calculations show strong exciton absorption at 2.3 eV in InN NWs, approximately. We thus believe that the well-known band gap controversy of InN from 0.6 to 2.3 eV[39] is probably caused by quantum confinement of these surface microwire structures.

Let us now discuss the origin of the broadening YL band centered at 2.2 eV. The PL spectra from Ga-rich to N-rich conditions are shown in Figure 6a, by which an obvious YL enhancement can be found under the N-rich condition. The strong broadening emission band indicates Ga vacancy should be one major contributor to YL owing to its easy formation under the N-rich condition.[40] In fact, direct evidence for the correlation between Ga vacancy and YL in GaN has emerged from positron annihilation measurements by Saarinen and co-workers.[41] They observed an enhancement of the YL due to the increasing concentration of Ga

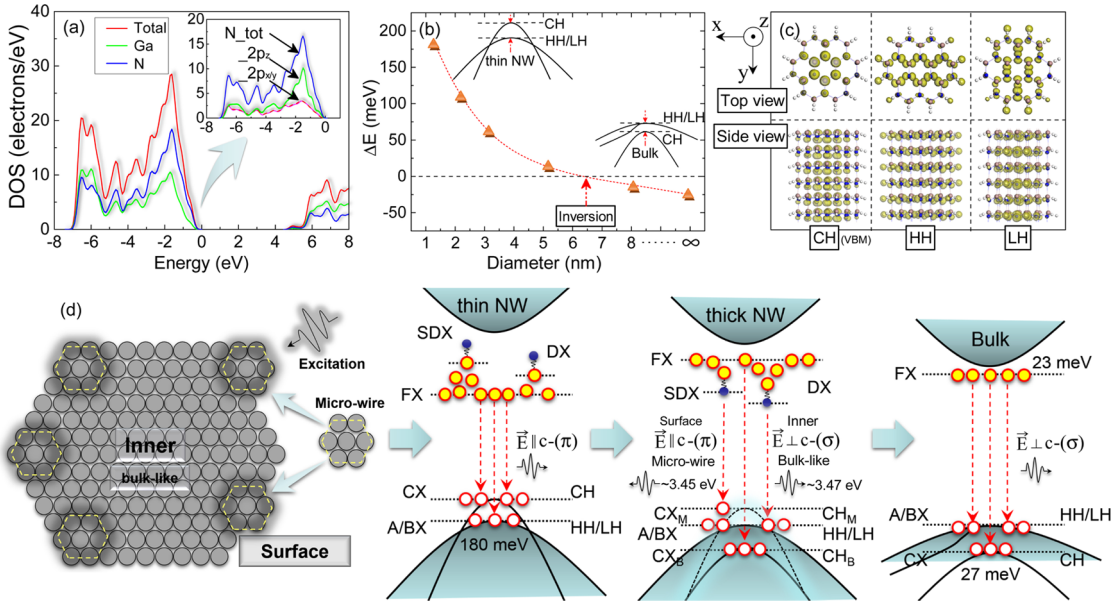

Figure 5. Partial density of states for GaN NWs (a). Energy of the valence band inversion ΔE from CH to HH/LH bands (b). Isosurface charge density distributions ($\rho = 0.03 e$Å^{-3}) at the top of the three valence bands (c). Schematic representation of the surface microwire in the self-assembled GaN NWs and the corresponding optical transition mechanism from thin to thick GaN NWs (d). On the basis of previous work[15] and our calculations, we show the exciton energy levels of donor bound (DX), surface donor bound (SDX), and free (FX) excitons and the corresponding optical transitions of A, B, and C excitons (AX, BX, and CX). The subscript M and B indicate microwire and bulk-like, respectively.

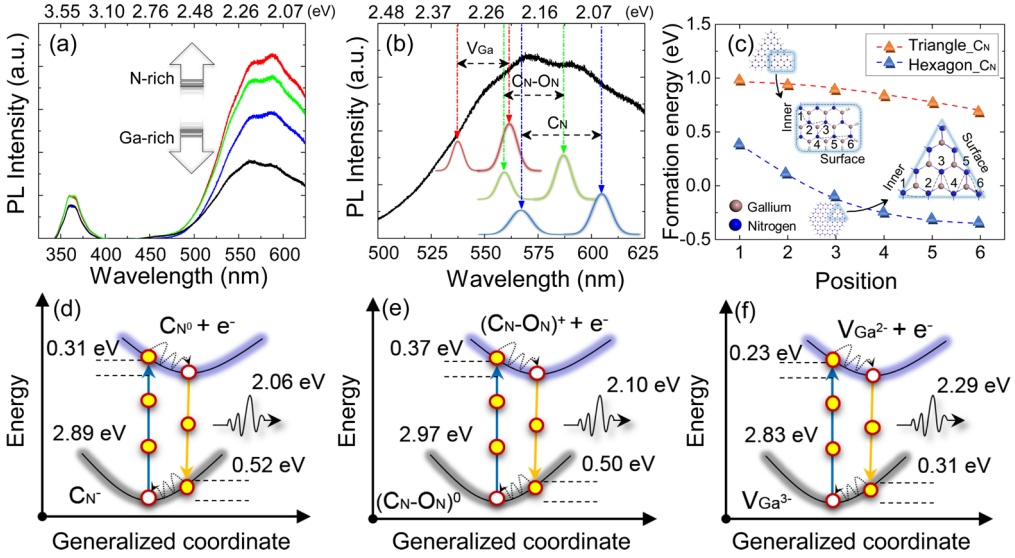

Figure 6. PL of GaN NWs under different growth conditions from N-rich to Ga-rich (a). Broadening YL band determined by V_{Ga}, C_N and C_N-O_N defects (b). Formation energy of C_N defect in trianglar and hexagonal GaN NWs (c). The configuration diagrams illustrate the different absorptions and emissions in GaN NWs for C_N (d), C_N-O_N (e), and V_{Ga} (f) defects.

vacancies from 10^{17} to 10^{18} cm^{-3}. Li and Wang[16] also suggested the surface Ga vacancies as the origin of the YL band in GaN NWs. In addition to Ga vacancy, the carbon-related defects are also the most likely to be introduced because of trimethylgallium adopted during the self-assembled growth. There has been strong evidence that the carbon-related defects C_N and C_N-O_N can exist stably in GaN with formation energy lower than that of the others, such as C_{Ga}.[23]

As stated above, we believe there is a close similarity of the existing defects between GaN bulk and NWs. The only difference is the environment from the NW interior to surface. Our calculated formation energy (see Figure 6c) reveals that the C_N defects tend to gather around the NW side wall. A similar result also holds for vacancies.[42] If these defects exist in the interior of the NW, they will need extra energy to break down the inner perfect crystal structure and the whole system requires a large lattice relaxation. The above conclusion has been supported by previous experiments.[16] It has been known that V_{Ga}, C_N, and C_N-O_N can exist stably with definite charge states in GaN as acceptors.[21,23,43]

Similarly, these charged defects are easily formed at the NW surface layer because of their lower formation energy. The optical transitions related to these defects are presented in Figure 6d–f, in which the strong excitonic effect in 1D NWs has been taken into account. The calculated ionization energies (0.51, 0.44, and 0.37 eV) of V_{Ga}, C_N, and C_N–O_N defects at the NW side wall are significantly lower than their corresponding values for the inner bulk-like defects (1.1, 0.9, and 0.76 eV),[21,23,43] which is consistent with the tight binding results.[44] As a result of the optical excitation producing electron–hole (e–h) pairs, the enhanced e–h interaction can form strongly bound excitons along the NW axis. Loosing the excess energy through the fast lattice-relaxation, the defects return to their initial states accompanied by photon emission. Our calculations indicate that the optical transition energies for V_{Ga}, C_N, and C_N–O_N are in the YL region (see Figure 6d–f). The different distributions of these defects at the NW surface layer cause an energy shift from 2.06 to 2.29 eV, resulting in a Gaussian smearing of the YL band (see Figure 6b).

We can thus confirm from the above analyses that the broadening YL band in GaN NWs is caused by gallium vacancies and carbon impurities distributed at the surface layer of GaN NWs. The physical reasons can be summarized as follows. (i) The YL band can not be caused by a single defect because of its large bandwidth from 525 to 625 nm. (ii) It is known that the intrinsic vacancy defects are inevitable in epitaxial materials, and GaN NWs are no exception. Meanwhile, the carbon impurities should be introduced because of trimethylgallium adopted during the self-assembled growth of GaN NWs. In particular, these defects are inclined to assemble at the NW surface owing to their lower formation energy and less lattice distortion, which is why the surface layer exhibits strong YL in ref 16. (iii) From Ga-rich to N-rich conditions, the YL of GaN NWs becomes more and more significant, which manifests that the increasing concentration of gallium vacancy is beneficial to YL owing to its easier formation under the N-rich conditions. (iv) Compared with the self-assembled GaN NWs fabricated by MOCVD with trimethylgallium, our high-quality MBE-grown GaN NWs with metal gallium are YL-free (Supporting Information Figure 1). Moreover, our energy dispersive spectrometry (EDS) measurements clearly indicate the absence of carbon impurities in MBE-grown GaN NWs. The strong YL is thus closely related to the carbon defects. (v) Our calculated optical transition energies of gallium vacancy and carbon impurities distributed at the GaN NW surface layer almost cover the full range of the broadening YL band, which confirms the domination of these defects in YL.

It is worth noting that, as we mentioned above, the nature of the broadening YL band is due to the existence of the gallium vacancy and carbon impurities at the surface layer of GaN NWs. These defects tend to migrate to the NW surface owing to the demand of stress release, which is necessary to guarantee the stability of the whole structure with the lowest energy and independent of the NW shapes. Our theoretical explanation for the broadening YL band is thus universal and suitable for the GaN NWs with any shape.

CONCLUSIONS

On the basis of the advanced first-principles calculations with many-body perturbation theory and polarization-resolved experiments, we resolve two long-debated issues in GaN NWs. We prove that the surface microwire or microstructure with amazing characteristics, widely existing in epitaxially grown samples, is profound and provides new insights into some controversial puzzles. We find that 1D quantum confinement in small diameter GaN NWs significantly increases the band gap to 4.85 eV and leads to a large exciton binding energy (~1.51 eV). The inversion of the top valence bands in the decreasing order of the CH and HH/LH bands becomes more and more significant with the decreasing NW diameter, which directly leads to the emitted photons polarized along the NW axis. The optical transition from bound excitons localized around the surface microwire to CH band is the essence of the observed 3.45 eV emission line with $\mathbf{E} \parallel c$ polarization, which is different from the DX(A) line (3.47 eV) with $\mathbf{E} \perp c$ polarization. The puzzle debated for 15 years is thus completely revealed. As acceptors, V_{Ga}, C_N, and C_N–O_N tend to assemble at the NW side wall. Moreover, the optical transition energies related to these defects are in the YL region. The different distributions of these defects at the NW surface layer result in a Gaussian smearing of the YL band, which is in excellent agreement with our PL data. We thus clarify the physical origin of the 3.45 eV emission line (YL band) related to surface microwire (defects) in GaN NWs, which is quite useful for understanding the luminescence mechanism and improving the optical performance of GaN NW-based optoelectronic nanodevices. We believe our proposed surface microwire or microstructure is critical to resolving previous intense debates, such as the unresolved puzzle of the InN gap.

MATERIALS AND METHODS

Synthesis of GaN Nanowires. Self-assembled growth of catalyst-free GaN nanowires is carried out at high pressure in a commercial 3 × 2 in. MOVPE close-coupled showerhead reactor (CS12014) on *c*-plane sapphire substrates. Trimethylgallium (TMG), ammonia (NH_3), and silane (100 ppm diluted in H_2) are the precursors for Ga, N, and Si, respectively. First, the substrate is baked *in situ* under H_2 atmosphere at 1040 °C for 20 min and nitridated using NH_3 with a 2000 sccm flow for 120 s to form a thin surface layer of AlN. The SiN_x deposition is performed by

injecting simultaneously SiH_4 (45 sccm) and NH_3 (4000 sccm) into the reactor at a pressure of 75 Torr. Second, a short GaN nucleation is performed on SiN_x by injecting TMG (65 sccm) and NH_3 (200 sccm) simultaneously into the reactor chamber under N_2/H_2 (1:1) carrier gas flow (2000 sccm) at 1000 °C. Finally, the system is directly switched to the wire growth process keeping the temperature at 1040 °C, NH_3 (200 sccm) and TMG (65 sccm) flows in N_2/H_2 carrier gas mixture (1:1) at a pressure of 200 Torr, and under additional injection of silane (45 sccm).

DFT and GW Calculations. The theoretical calculations are based on density functional theory (DFT) performed by using the VASP code.[45] During our DFT calculations, enough *k*-point sampling ($1 \times 1 \times 6$) is used for the structure relaxation. The generalized gradient approximation (GGA) with Perdew, Burke, and Ernzerhof (PBE) functional is adopted.[46] The Ga ($4s^2 4p^1 3d^{10}$), N ($2s^2 2p^3$), and H ($1s^1$) are considered as valence electrons. Energy cutoff is set to 500 eV, and structural optimization is carried out until the maximum energy difference and residual forces converge to 10^{-5} eV and 0.01 eV/Å. In our DFT-1/2 scheme,[26,27] the half ionization is applied to the p-orbital of N atom. Both CUT and *n* parameters are tested by means of a comparison with experimental band gap of GaN. We adopt $n = 8$ and CUT = 2.75 for N atom to calculate the band gaps of GaN bulk and NWs. The GW correction and Bethe–Salpeter equation calculations are carried out in BerkeleyGW package.[47] For the quasiparticle calculations performed with the BerkeleyGW code, the ground-state Kohn–Sham wave functions and eigenvalues are obtained using a local density approximation (LDA) exchange-correlation functional with Troullier–Martins norm-conserving pseudopotentials,[48,49] as implemented in Quantum Espresso code.[50] A kinetic energy cutoff of 150 Ry is used for the wave function. To eliminate the interaction between periodic images of NWs in adjacent supercells, the lateral dimensions are chosen to be 30 Å. During the GW calculations, we choose $1 \times 1 \times 8$ *k*-point mesh, which yields quasiparticle energies converged within ±0.1 eV. To perform the Bethe–Salpeter equation calculations, we interpolate the electron–hole interaction kernel on a $1 \times 1 \times 24$ *k*-point mesh. This choice of parameters yields well-converged exciton eigenenergies and sufficient accuracy in our GaN NW calculations.

Defect Formation Energy. The defect formation energy is simply the reaction energy to create a defect from ideal structure, which depends on the growth or annealing conditions. The defect formation energy, E_f, of defect α in the charge state *q* can be calculated as follows:

$$E_f(\alpha, q) = E_{NW}(\alpha, q) - E_{NW}(\text{perfect}) - \sum_i n_i \mu_i + qE_V + qE_F$$

where $E_{NW}(\alpha,q)$ is the total energy of a GaN NW containing a defect (V_{Ga}, C_N, or C_N–O_N) in charge state *q*; E_{NW}(perfect) is the total energy of the NW without defects; n_i is the atom number of the *i*th constituent, which has been added to ($n_i > 0$) or removed from ($n_i < 0$) the perfect NW; and μ_i is the corresponding chemical potential. E_F is the Fermi level referenced to the VBM E_V of the NW.

Optical Transition Energy. The optical transition related to the charged defect can be calculated by using the following formula:

$$E_{PL} = E_{exec} - E_{re1} - E_{re2}$$

where E_{exec} is the external excitation energy, which can be determined by the energy difference between the exciton energy and the defect level,[51] and E_{re1} and E_{re2} are structure relaxation energies at the initial and final defect states with different charges.

Conflict of Interest: The authors declare no competing financial interest.

Acknowledgment. This work was supported by the National Basic Research Program of China (2012CB619304) and the National Natural Science Foundation of China (11474012, 11364030, 11404013, 61204013). We used computational resources of the "Explorer 100" cluster system of Tsinghua National Laboratory for Information Science and Technology.

Supporting Information Available: The Supporting Information is available free of charge on the ACS Publications website at DOI: 10.1021/acsnano.5b04158.

SEM images of GaN NWs fabricated by MBE, PL spectra of GaN NWs with different gallium sources, EDS measurement of GaN NWs, imaginary part of the dielectric function ε_2 for triangular GaN NWs, isosurface charge density distributions at the top of the three valence bands for GaN bulk, and electronic band structures of GaN bulk and surface microwire (PDF)

REFERENCES AND NOTES

1. Guo, W.; Zhang, M.; Banerjee, A.; Bhattacharya, P. Catalyst-Free InGaN/GaN Nanowire Light Emitting Diodes Grown on (001) Silicon by Molecular Beam Epitaxy. *Nano Lett.* **2010**, *10*, 3355–3359.
2. Qian, F.; Li, Y.; Gradečak, S.; Park, H. G.; Dong, Y.; Ding, Y.; Wang, Z. L.; Lieber, C. M. Multi-Quantum-Well Nanowire Heterostructures for Wavelength-Controlled Lasers. *Nat. Mater.* **2008**, *7*, 701–706.
3. Li, Y.; Xiang, J.; Qian, F.; Gradecak, S.; Wu, Y.; Yan, H.; Blom, D. A.; Lieber, C. M. Dopant-Free GaN/AlN/AlGaN Radial Nanowire Heterostructures as High Electron Mobility Transistors. *Nano Lett.* **2006**, *6*, 1468–1473.
4. Dahal, R.; Li, J.; Aryal, K.; Lin, J. Y.; Jiang, H. X. InGaN/GaN Multiple Quantum Well Concentrator Solar Cells. *Appl. Phys. Lett.* **2010**, *97*, 073115.
5. Schmidt, V.; Gösele, U. How Nanowires Grow. *Science* **2007**, *316*, 698.
6. Tomioka, K.; Motohisa, J.; Hara, S.; Fukui, T. Control of InAs Nanowire Growth Directions on Si. *Nano Lett.* **2008**, *8*, 3475–3480.
7. Thillosen, N.; Sebald, K.; Hardtdegen, H.; Meijers, R.; Calarco, R.; Montanari, S.; Kaluza, N.; Gutowski, J.; Lüth, H. The State of Strain in Single GaN Nanocolumns as Derived from Micro-Photoluminescence Measurements. *Nano Lett.* **2006**, *6*, 704–708.
8. Calleja, E.; Sanchez-Garcia, M. A.; Sanchez, F. J.; Calle, F.; Naranjo, F. B.; Munoz, E.; Jahn, U.; Ploog, K. Luminescence Properties and Defects in GaN Nanocolumns Grown by Molecular Beam Epitaxy. *Phys. Rev. B: Condens. Matter Mater. Phys.* **2000**, *62*, 16826.
9. Xu, S.; Hao, Y.; Zhang, J.; Jiang, T.; Yang, L.; Lu, X.; Lin, Z. Yellow Luminescence of Polar and Nonpolar GaN Nanowires on r-Plane Sapphire by Metal Organic Chemical Vapor Deposition. *Nano Lett.* **2013**, *13*, 3654–3657.
10. Sam-Giao, D.; Mata, R.; Tourbot, G.; Renard, J.; Wysmolek, A.; Daudin, B.; Gayral, B. Fine Optical Spectroscopy of the 3.45 eV Emission Line in GaN Nanowires. *J. Appl. Phys.* **2013**, *113*, 043102.
11. Corfdir, P.; Lefebvre, P.; Ristić, J.; Valvin, P.; Calleja, E.; Trampert, A.; Ganiere, J. D.; Deveaud-Plédran, B. Time-Resolved Spectroscopy on GaN Nanocolumns Grown by Plasma Assisted Molecular Beam Epitaxy on Si Substrates. *J. Appl. Phys.* **2009**, *105*, 013113.
12. Robins, L. H.; Bertness, K. A.; Barker, J. M.; Sanford, N. A.; Schlager, J. B. Optical and Structural Study of GaN Nanowires Grown by Catalyst-Free Molecular Beam Epitaxy. I. Near-Band-Edge Luminescence and Strain Effects. *J. Appl. Phys.* **2007**, *101*, 113505.
13. Furtmayr, F.; Vielemeyer, M.; Stutzmann, M.; Laufer, A.; Meyer, B. K.; Eickhoff, M. Optical Properties of Si-and Mg-Doped Gallium Nitride Nanowires Grown by Plasma-Assisted Molecular Beam Epitaxy. *J. Appl. Phys.* **2008**, *104*, 074309.
14. Lefebvre, P.; Fernández-Garrido, S.; Grandal, J.; Ristić, J.; Sánchez-García, M. A.; Calleja, E. Radiative Defects in GaN Nanocolumns: Correlation with Growth Conditions and Sample Morphology. *Appl. Phys. Lett.* **2011**, *98*, 083104.
15. Brandt, O.; Pfüller, C.; Chèze, C.; Geelhaar, L.; Riechert, H. Sub-meV Linewidth of Excitonic Luminescence in Single GaN Nanowires: Direct Evidence for Surface Excitons. *Phys. Rev. B: Condens. Matter Mater. Phys.* **2010**, *81*, 045302.
16. Li, Q.; Wang, G. T. Spatial Distribution of Defect Luminescence in GaN Nanowires. *Nano Lett.* **2010**, *10*, 1554–1558.
17. Li, S.; Waag, A. GaN Based Nanorods for Solid State Lighting. *J. Appl. Phys.* **2012**, *111*, 071101.

18. Wang, G. T.; Talin, A. A.; Werder, D. J.; Creighton, J. R.; Lai, E.; Anderson, R. J.; Arslan, I. Highly Aligned, Template-Free Growth and Characterization of Vertical GaN Nanowires on Sapphire by Metal-Organic Chemical Vapour Deposition. *Nanotechnology* **2006**, *17*, 5773.
19. Seager, C. H.; Wright, A. F.; Yu, J.; Gotz, W. Role of Carbon in GaN. *J. Appl. Phys.* **2002**, *92*, 6553.
20. Ogino, T.; Aoki, M. Mechanism of Yellow Luminescence in GaN. *Jpn. J. Appl. Phys.* **1980**, *19*, 2395.
21. Neugebauer, J.; Van de Walle, C. G. Gallium Vacancies and the Yellow Luminescence in GaN. *Appl. Phys. Lett.* **1996**, *69*, 503–505.
22. Mattila, T.; Nieminen, R. M. Point-Defect Complexes and Broadband Luminescence in GaN and AlN. *Phys. Rev. B: Condens. Matter Mater. Phys.* **1997**, *55*, 9571.
23. Demchenko, D. O.; Diallo, I. C.; Reshchikov, M. A. Yellow Luminescence of Gallium Nitride Generated by Carbon Defect Complexes. *Phys. Rev. Lett.* **2013**, *110*, 087404.
24. Avit, G.; Lekhal, K.; André, Y.; Bougerol, C.; Réveret, F.; Leymarie, J.; Gil, E.; Monier, G.; Castelluci, D.; Trassoudaine, A. Ultralong and Defect-Free GaN Nanowires Grown by the HVPE Process. *Nano Lett.* **2014**, *14*, 559–562.
25. Hybertsen, M.; Louie, S. G. Electron Correlation in Semiconductors and Insulators: Band Gaps and Quasiparticle Energies. *Phys. Rev. B: Condens. Matter Mater. Phys.* **1986**, *34*, 5390.
26. Ferreira, L. G.; Marques, M.; Teles, L. K. Approximation to Density Functional Theory for the Calculation of Band Gaps of Semiconductors. *Phys. Rev. B: Condens. Matter Mater. Phys.* **2008**, *78*, 125116.
27. Ferreira, L. G.; Marques, M.; Teles, L. K. Slater Half-Occupation Technique Revisited: the LDA-1/2 and GGA-1/2 Approaches for Atomic Ionization Energies and Band Gaps in Semiconductors. *AIP Adv.* **2011**, *1*, 032119.
28. Heyd, J.; Scuseria, G. E.; Ernzerhof, M. Hybrid Functionals Based on a Screened Coulomb Potential. *J. Chem. Phys.* **2003**, *118*, 8207.
29. Hedin, L.; Lundqvist, S. Effects of Electron-Electron and Electron-Phonon Interactions on the One-Electron States of Solids. *Solid State Phys.* **1970**, *23*, 1.
30. Rubio, A.; Corkill, J. L.; Cohen, M. L.; Shirley, E. L.; Louie, S. G. Quasiparticle Band Structure of AlN and GaN. *Phys. Rev. B: Condens. Matter Mater. Phys.* **1993**, *48*, 11810.
31. Monemar, B. Fundamental Energy Gap of GaN from Photoluminescence Excitation Spectra. *Phys. Rev. B* **1974**, *10*, 676.
32. Morkoc, H.; Strite, S.; Gao, G. B.; Lin, M. E.; Sverdlov, B.; Burns, M. Large-Band-Gap SiC, III-V Nitride, and II-VI ZnSe-Based Semiconductor Device Technologies. *J. Appl. Phys.* **1994**, *76*, 1363–1398.
33. Wang, Z.; Li, J.; Gao, F.; Weber, W. J. Codoping of Magnesium with Oxygen in Gallium Nitride Nanowires. *Appl. Phys. Lett.* **2010**, *96*, 103112.
34. Shan, W.; Little, B. D.; Fischer, A. J.; Song, J. J.; Goldenberg, B.; Perry, W. G.; Bremser, M. D.; Davis, R. F. Binding Energy for the Intrinsic Excitons in Wurtzite GaN. *Phys. Rev. B: Condens. Matter Mater. Phys.* **1996**, *54*, 16369.
35. Molina-Sanchez, A.; García-Cristóbal, A. Anisotropic Optical Response of GaN and AlN Nanowires. *J. Phys.: Condens. Matter* **2012**, *24*, 295301.
36. Dimakis, E.; Iliopoulos, E.; Tsagaraki, K.; Georgakilas, A. Physical Model of InN Growth on Ga-Face GaN (0001) by Molecular-Beam Epitaxy. *Appl. Phys. Lett.* **2005**, *86*, 133104.
37. Motlan; Goldys, E. M.; Tansley, T. L. The Effect of Target Nitridation on Structural Properties of InN Grown by Radio-Frequency Reactive Sputtering. *Thin Solid Films* **2002**, *422*, 28–32.
38. Himmerlich, M.; Krischok, S.; Lebedev, V.; Ambacher, O.; Schaefer, J. A. Morphology and Surface Electronic Structure of MBE Grown InN. *J. Cryst. Growth* **2007**, *306*, 6–11.
39. Butcher, K. S. A.; Tansley, T. L. InN, Latest Development and a Review of the Band-Gap Controversy. *Superlattices Microstruct.* **2005**, *38*, 1–37.
40. Neugebauer, J.; Van de Walle, C. G. Atomic Geometry and Electronic Structure of Native Defects in GaN. *Phys. Rev. B: Condens. Matter Mater. Phys.* **1994**, *50*, 8067.
41. Saarinen, K.; Laine, T.; Kuisma, S.; Nissilä, J.; Hautojärvi, P.; Dobrzynski, L.; Baranowski, J. M.; Pakula, K.; Stepniewski, R.; Wojdak, M.; et al. Observation of Native Ga Vacancies in GaN by Positron Annihilation. *Phys. Rev. Lett.* **1997**, *79*, 3030.
42. Wang, Z.; Li, J.; Gao, F.; Weber, W. J. Defects in Gallium Nitride Nanowires: First Principles Calculations. *J. Appl. Phys.* **2010**, *108*, 044305.
43. Lyons, J. L.; Janotti, A.; van de Walle, C. G. Carbon Impurities and the Yellow Luminescence in GaN. *Appl. Phys. Lett.* **2010**, *97*, 152108.
44. Diarra, M.; Niquet, Y. M.; Delerue, C.; Allan, G. Ionization Energy of Donor and Acceptor Impurities in Semiconductor Nanowires: Importance of Dielectric Confinement. *Phys. Rev. B: Condens. Matter Mater. Phys.* **2007**, *75*, 045301.
45. Kresse, G.; Furthmüller, J. Efficiency of Ab-Initio Total Energy Calculations for Metals and Semiconductors Using a Plane-Wave Basis Set. *Comput. Mater. Sci.* **1996**, *6*, 15.
46. Perdew, J. P.; Burke, K.; Ernzerhof, M. Generalized Gradient Approximation Made Simple. *Phys. Rev. Lett.* **1996**, *77*, 3865–3868.
47. Deslippe, J.; Samsonidze, G.; Strubbe, D. A.; Jain, M.; Cohen, M. L.; Louie, S. G. BerkeleyGW: A Massively Parallel Computer Package for the Calculation of the Quasiparticle and Optical Properties of Materials and Nanostructures. *Comput. Phys. Commun.* **2012**, *183*, 1269.
48. Ceperley, D. M.; Alder, B. J. Ground State of the Electron Gas by a Stochastic Method. *Phys. Rev. Lett.* **1980**, *45*, 566.
49. Perdew, J. P.; Zunger, A. Self-Interaction Correction to Density-Functional Approximations for Many-Electron Systems. *Phys. Rev. B: Condens. Matter Mater. Phys.* **1981**, *23*, 5048.
50. Giannozzi, P.; Baroni, S.; Bonini, N.; Calandra, M.; Car, R.; Cavazzoni, C.; Ceresoli, D.; Chiarotti, G. L.; Cococcioni, M.; Dabo, I.; et al. QUANTUM ESPRESSO: a Modular and Open-Source Software Project for Quantum Simulations of Materials. *J. Phys.: Condens. Matter* **2009**, *21*, 395502.
51. Lyons, J. L.; Janotti, A.; Van de Walle, C. G. Shallow *Versus* Deep Nature of Mg Acceptors in Nitride Semiconductors. *Phys. Rev. Lett.* **2012**, *108*, 156403.